Title

Carbohydrate-Dependent Binding of Langerin to SodC, a Cell Wall Glycoprotein of Mycobacterium leprae

Journal

Journal of Bacteriology, 197(3)

ISSN

0021-9193

Authors

Kim, Hee Jin
Brennan, Patrick J
Heaslip, Darragh
et al.

Publication Date

2015-02-01

DOI

10.1128/jb.02080-14

Peer reviewed

JB
Journals.ASM.org

Carbohydrate-Dependent Binding of Langerin to SodC, a Cell Wall Glycoprotein of *Mycobacterium leprae*

Hee Jin Kim,[a] Patrick J. Brennan,[a] Darragh Heaslip,[a] Mark C. Udey,[b] Robert L. Modlin,[c] John T. Belisle[a]

Mycobacteria Research Laboratories, Department of Microbiology, Immunology and Pathology, Colorado State University, Fort Collins, Colorado, USA[a]; Center for Cancer Research, National Cancer Institute, National Institutes of Health, Bethesda, Maryland, USA[b]; Division of Dermatology and Department of Microbiology, Immunology and Molecular Genetics, David Geffen School of Medicine at the University of California, Los Angeles, California, USA[c]

Langerhans cells participate in the immune response in leprosy by their ability to activate T cells that recognize the pathogen, *Mycobacterium leprae*, in a langerin-dependent manner. We hypothesized that langerin, the distinguishing C-type lectin of Langerhans cells, would recognize the highly mannosylated structures in pathogenic *Mycobacterium* spp. The coding region for the extracellular and neck domain of human langerin was cloned and expressed to produce a recombinant active trimeric form of human langerin (r-langerin). Binding assays performed in microtiter plates, by two-dimensional (2D) Western blotting, and by surface plasmon resonance demonstrated that r-langerin possessed carbohydrate-dependent affinity to glycoproteins in the cell wall of *M. leprae*. This lectin, however, yielded less binding to mannose-capped lipoarabinomannan (ManLAM) and even lower levels of binding to phosphatidylinositol mannosides. However, the superoxide dismutase C (SodC) protein of the *M. leprae* cell wall was identified as a langerin-reactive ligand. Tandem mass spectrometry verified the glycosylation of a recombinant form of *M. leprae* SodC (rSodC) produced in *Mycobacterium smegmatis*. Analysis of r-langerin affinity by surface plasmon resonance revealed a carbohydrate-dependent affinity of rSodC (equilibrium dissociation constant [K_D] = 0.862 μM) that was 20-fold greater than for *M. leprae* ManLAM (K_D = 18.69 μM). These data strongly suggest that a subset of the presumptively mannosylated *M. leprae* glycoproteins act as ligands for langerin and may facilitate the interaction of *M. leprae* with Langerhans cells.

Mycobacterium leprae infections lead to human leprosy, characterized by disfiguring skin lesions, nerve damage, and eventually permanent disability (1). As part of the disease process, *M. leprae* is phagocytized by numerous cell types, including dendritic cells (DCs) and epidermal DCs known as Langerhans cells (LCs) (2–4). The cell envelopes of pathogenic *Mycobacterium* spp., including *M. leprae*, are rich in mannosylated macromolecules such as mannose-capped lipoarabinomannan (ManLAM), lipomannan (LM), phosphatidylinositol mannosides (PIM) and presumably glycoproteins (5, 6). These glycoconjugates contribute to the interaction of pathogenic mycobacteria with host phagocytes, and the C-type lectin receptors (CLRs) that decorate the surface of phagocytes have been shown to directly bind specific mannosylated glycoconjugates of *Mycobacterium* spp (7). For DCs, the constitutive CLRs are the mannose receptor (CD206) and the dendritic cell-specific intracellular adhesion molecule-grabbing nonintegrin (DC-SIGN; CD209). However, langerin (CD207) is a CLR specific to LCs.

DC-SIGN and langerin recognize the sugar residues of macromolecules produced by pathogens and altered self-antigens in a calcium-dependent manner. These CLRs are comprised of a short cytoplasmic domain, a transmembrane domain, and, on the outer surface of the cell, an extracellular domain (ECD) that encompasses the highly conserved carbohydrate recognition domains (CRDs) and the hydrophobic neck domain. The CRDs determine sugar-binding specificity, and DC-SIGN and langerin possess an EPN (Glu-Pro-Asn) motif that is generally specific to oligosaccharides containing mannose (Man), fucose, glucose, or *N*-acetylglucosamine residues (8). The α-helix coiled-coil formation in the neck domains is responsible for the trimeric and tetrameric structures of langerin and DC-SIGN, respectively, and these multimeric conformations promote carbohydrate spatial specificity (9, 10). Some of mycobacterial ligands of DC-SIGN have been defined. Specifically, DC-SIGN recognizes the α(1→2) linkages of ManLAM and PIM_6 (11, 12). The 45-kDa and 19-kDa glycoproteins of *Mycobacterium tuberculosis* are also DC-SIGN ligands based on their inhibition of bacterial cell uptake via DC-SIGN-transfected cell lines (13). However, it should be noted that studies to directly compare the binding affinity of protein and lipoglycan ligands for C-type lectins or to define the relative contribution of each ligand have not been performed.

We previously demonstrated that langerin-positive LCs present cell wall antigens of *M. leprae* to CD1a-restricted T cells, resulting in T cell proliferation and gamma interferon (IFN-γ) production (2). This study demonstrated the biological significance for the interaction of *M. leprae* ligands with the langerin of LCs; however, the *M. leprae* binding partners of this CLR were not elucidated. Thus, in the present work we sought to characterize the biochemical and biophysical features of the *M. leprae* glycoconjugates recognized by langerin.

Received 12 July 2014 **Accepted** 20 November 2014

Accepted manuscript posted online 24 November 2014

Citation Kim HJ, Brennan PJ, Heaslip D, Udey MC, Modlin RL, Belisle JT. 2015. Carbohydrate-dependent binding of langerin to SodC, a cell wall glycoprotein of *Mycobacterium leprae*. J Bacteriol 197:615–625. doi:10.1128/JB.02080-14.

Editor: O. Schneewind

Address correspondence to John T. Belisle, john.belisle@colostate.edu.

Supplemental material for this article may be found at http://dx.doi.org/10.1128/JB.02080-14.

doi:10.1128/JB.02080-14

M. leprae is an obligate intracellular pathogen incapable of growth beyond the armadillo or nude mouse footpad; without a facile animal model to study mechanisms of infection, a robust *in vitro* approach is required to define the nature of *M. leprae* interactions with LCs. An *in vitro* CLR binding model using recombinant human langerin (r-langerin) was developed, which allowed the evaluation of langerin binding affinities for mycobacterial lipoglycans and glycoproteins. The data demonstrated that langerin poorly binds the known DC-SIGN ligands (ManLAM and PIM_6) but recognizes a specific set of *M. leprae* cell wall proteins, including SodC (ML1925). Recombinant production of the *M. leprae* SodC in *Mycobacterium smegmatis* allowed confirmation of SodC glycosylation, and evaluation of langerin binding kinetics demonstrated a carbohydrate-dependent affinity for SodC that was approximately 20-fold higher than that observed for *M. leprae* ManLAM.

MATERIALS AND METHODS

Preparation of mycobacterial fractions and ligands. *M. leprae* (200 mg) was purified from armadillo spleen (provided by Richard Truman, Louisiana State University) using the Draper protocol (14) and lysed by probe sonication. *M. leprae* cell wall antigen (MLCwA) was prepared from the whole-cell lysate by centrifugation at 27,000 × *g* and 4°C (15). The MLCwA was subjected to a TX-114 phase partitioning (16) to remove LAM, and the resulting aqueous phase was termed *M. leprae* cell wall antigen minus LAM [MLCwA(−)LAM].

M. tuberculosis and *M. leprae* ManLAM and PIM_6 were generated at Colorado State University (CSU) and supplied through the Biodefense and Emerging Infections (BEI) Research Resources Repository (http://www.beiresources.org/TBVTRMResearchMaterials/tabid/1431/Default.aspx).

Cloning, expression, and production of recombinant *M. leprae* SodC in *M. smegmatis* and *Escherichia coli*. To generate a fully glycosylated recombinant form of *M. leprae* SodC (rSodC), the *ml1925* gene was amplified by PCR using the forward primer CATATGTCTAAACTCGCCGGT and reverse primer AAGCTTGTCGGCGCCGATGAC (underlining indicates the NdeI and HindIII sites) and *M. leprae* Thai 53 genomic DNA as the template. The PCR products were digested with restriction enzymes and cloned into the *E. coli-M. smegmatis* shuttle expression vector pVV16 (17). The resulting recombinant plasmid, pMRLB101, was transformed into *M. smegmatis* mc^2155. The rSodC with a C-terminal 6×His tag was purified by immobilized metal affinity chromatography (IMAC) with nickel-nitrilotriacetic acid (Ni-NTA)–agarose resin (Qiagen) as described by Sieling et al. (17). Final purification of rSodC was achieved by preparative PAGE with a Nuphage 4 to 12% bis-Tris gel (Invitrogen Life Technologies, Carlsbad, CA) under denaturing conditions and gel elution by a mini-whole-gel eluter (WGE; Bio-Rad Life Science, Hercules, CA) (18). Eluted rSodC was desalted and concentrated in an Amicon Ultra-15 10 K centrifugal filter unit (Millipore, Bedford, MA).

A recombinant form of SodC lacking its signal peptide (rSodC-SP) was produced in *E. coli*. A fragment of *ml1925* was amplified by PCR using the forward primer CATATGAACCAACCCCCAGCGACCTT and reverse primer AAGCTTGCCGATGACACCGCACGCTA. The 630-bp PCR product was ligated to pET28a(+) to yield pMRLB102. The rSodC-SP was purified as described by Kim et al. (19) and sent to Lampire (Everett, PA) for generation of rabbit anti-SodC polyclonal sera.

Preparation of soluble recombinant langerin. The ECD coding region of human langerin was recovered from the pET30:langerin construct (20) by digestion with BamHI and HindIII and ligated into the *E. coli* expression vector pET28a(+) to yield pMRLB103. Two synthetic oligonucleotides (5′-TATG**GACTACAAGGATGACGACGACAAG**CCAGATCTGGGTACCGCCATGGCTGATATCG-3′ for the sense strand and 5′-TG**GACTACAAGGATGACGACGACAAG**CCAGATCTGGGTACCGCCATGGCTGATATCGGATC-3′ for the antisense strand) encoding the FLAG peptide (bold) were mixed in TE buffer (10 mM Tris-HCl [pH 7.4], 1 mM EDTA) at 25 μM, heated at 100°C for 5 min, annealed at room temperature for 3 h, and ligated into pMRLB103. This resulted in the recombinant plasmid pMRLB104, which encoded the ECD of human langerin with N-terminal 6×His and FLAG tags. The soluble r-langerin was purified from the *E. coli* BL21 Star (DE3) pLysS expression system and refolded as described by Stambach and Taylor (10).

Langerin binding assays. Prior to use of r-langerin in binding assays, its functionality was confirmed based on Ca^{2+}-dependent binding and sugar specificity of soybean agglutinin, as described in the supplemental text and demonstrated in Fig. S1 in the supplemental material. Additionally, a steady-state affinity model established the equilibrium dissociation constant (K_D) of r-langerin with yeast invertase and soybean agglutinin (see the supplemental text and Fig. S2 in the supplemental material).

Immobilized-ligand lectin binding (ILB) assay. Aliquots (100 μl) of agglutinin, yeast invertase, MLCwA, MLCwA(−)LAM, PIM_6, and *M. tuberculosis* and *M. leprae* ManLAM at 0.5 μg/ml in 0.1 M sodium carbonate (pH 9.6) were used to coat polystyrene Immulon IV 96-well enzyme-linked immunosorbent assay (ELISA) plates (Dynex Technologie) in duplicate (21). The wells were blocked with 2% bovine serum albumin (BSA) in TBST. After a washing with TBST, each well was incubated with 100 μl of 2 μg/ml r-langerin with 5 mM $CaCl_2$ or 2 mM EDTA at 37°C for 1 h. To verify the efficiency of mycobacterial ligand coating of the microtiter plate wells, a parallel assay was performed with horseradish peroxidase (HRP)-conjugated concanavalin A (ConA) (0.5 μg/ml) as the lectin probe. For inhibition assays, r-langerin was incubated with 100 mM galactose, glucose, or mannose or 100 μg/ml of mannan in 5 mM $CaCl_2$ prior to addition to the well. Anti-FLAG monoclonal antibody (MAb) M2 conjugated with HRP (Sigma-Aldrich) at a 1:20,000 dilution was used as the secondary probe to assess r-langerin binding. Peroxidase activity was detected by the addition of the 3,3′,5,5′-tetramethylbenzidine (TMB) (Sigma-Aldrich) substrate and measured by absorbance at 450 nm. Absorbance values were reported after subtracting the absorbance of the langerin control to which no ligand was added. One-way analysis of variance (ANOVA), followed by Tukey's multiple-means comparison test in GraphPad Prism 5.0 software (GraphPad Software, La Jolla, CA), was used to evaluate the statistical significance of langerin binding affinities for the mycobacterial ligands and controls.

SPR assay. Surface plasmon resonance binding (SPR) assays were performed with a Biacore T100 instrument (GE Healthcare) by the amine coupling method as described by Lozach et al. (22). The r-langerin (10 μg/ml) was immobilized on the activated CM5 sensor chip at a flow rate of 10 μl/min for a contact time of 420 s. Uncoupled amide groups in the flow cells were blocked with 130 μl of ethanolamine, pH 8.5. To correct the sample value, the reference cell of the CM5 sensor chip was processed by the same coupling procedure without addition of r-langerin. Binding assays were performed in HBS+P buffer (10 mM HEPES [pH 7.4], 150 mM NaCl, 0.005% surfactant P-20, 2 mM $CaCl_2$). Analytes were injected at various concentrations (5 to 6,400 nM or 0.5 to 100 μg/ml) at a flow rate of 10 μl/min for a contact time of 60 s. After each cycle, the r-langerin on the surface of sensor ship was regenerated with 300 mM methylmannopyranoside and 50 mM EDTA in HBS+P buffer. The SPR data under steady-state affinity conditions were analyzed to determine the equilibrium dissociation constant (K_D) using BIAevaluation software 2.02 (GE Healthcare). Scatchard plot analysis of SPR response values was performed to evaluate the binding efficiency by linear regression with the equation $R_{eq}/C = R_{max} \times C/(K_D + C)$ using GraphPad Prism 5.0 software. The response value at equilibrium (R_{eq}) was obtained for each analyte concentration (C) when the binding response became stabilized. R_{max} was the maximal analyte binding capacity of the surface, measured in resonance units (RU).

PAGE, 2D-PAGE, and Western blot analyses. rSodC (0.2 μg) was subjected to PAGE using Nuphage 4 to 12% bis-Tris polyacrylamide gels (Invitrogen Life Technologies) under denaturing conditions. MLCwA (150 μg) in 8 M urea, 2 M thiourea, 20 mM dithiothreitol (DTT), 4%

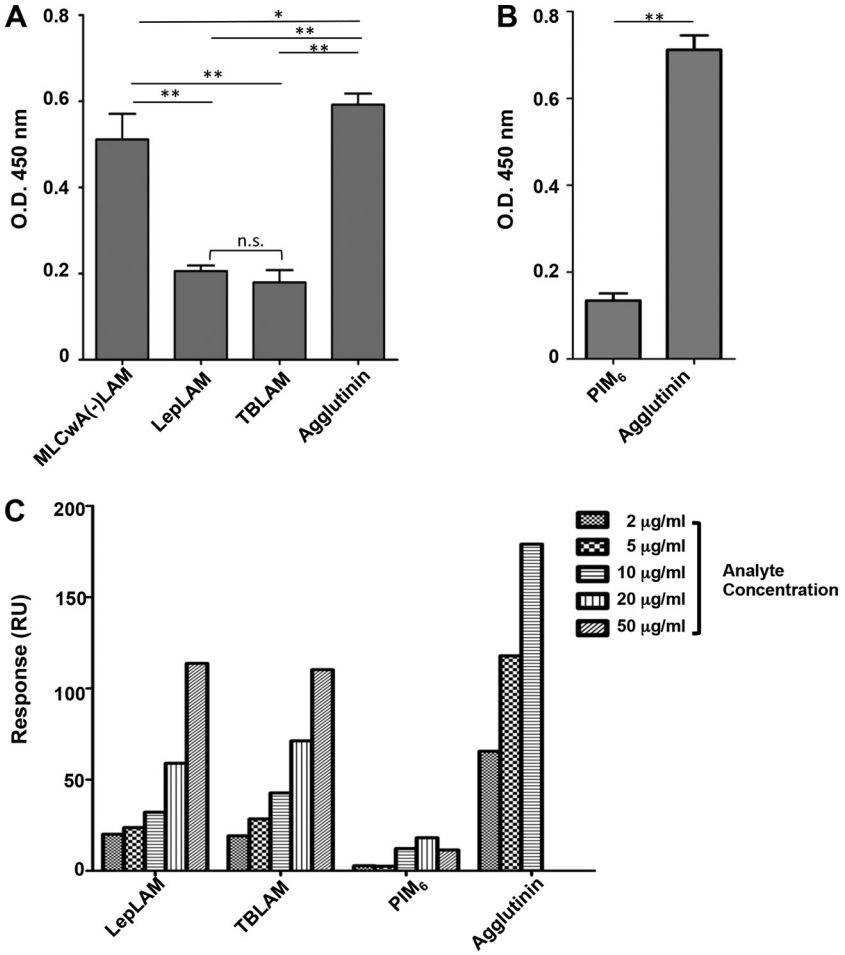

FIG 1 Evaluation of the properties of langerin binding to mycobacterial ligands. (A) r-langerin reactivity to mycobacterial protein preparations and ManLAM, assessed by ligand ELISA. The ligands (0.05 μg per well) were incubated with r-langerin (2 μg/ml) (8 independent assays). A one-way ANOVA combined with Tukey's multiple comparison analysis was performed to determine the statistical difference between each mycobacterial ligand and agglutinin. **, $P < 0.01$; *, $P < 0.05$. (B) Langerin reactivity of PIM_6, assessed by ligand ELISA (4 independent assays). (C) Dose response of *M. leprae* ManLAM (LepLAM), *M. tuberculosis* ManLAM (TBLAM), PIM_6, and agglutinin binding to immobilized r-langerin was measured by SPR. The data are representative of three independent SPR analyses.

(wt/vol) CHAPS {3-[(3-cholamidopropyl)-dimethylammonio]-1-propanesulfonate}, 1% (wt/vol) amidosulfobetaine 14 (ASB-14), 0.7% pH 4 to 7 ampholytes, and 0.3% pH 3 to 10 ampholytes was applied to Immobiline dry strips with pH gradients of 4 to 7. Isoelectric focusing (IEF) was performed with a Multiphore II unit (GE Healthcare) at 50 V, 100 V, 150 V, 200 V, 250 V, and 300 V sequentially for 6 min each, followed by 500 V for 12 min and 3,000 V for 5 h. Separation in the second dimension was achieved using Nuphage 4 to 12% bis-Tris SDS-polyacrylamide gels.

For Western blot analyses, proteins were transferred onto Immobilon polyvinylidene difluoride (PVDF) membranes (Millipore) and probed with the following: (i) r-langerin (5 μg/ml), 5 mM $CaCl_2$, and anti-FLAG M2 MAb as the secondary antibody; (ii) anti-SodC polyclonal sera with HRP-conjugated mouse anti-rabbit IgG as the secondary antibody; and (iii) HRP-conjugated ConA (5 μg/ml). The reactive spots were visualized by chemiluminescence using Supersignal West Dura substrate (Thermo Fischer Scientific) and the ChemiDoc XRS system (Bio-Rad Laboratories, Hercules, CA).

Protein mass spectrometry. Gel pieces corresponding to r-langerin and ConA-reactive spots were subjected to in-gel proteolytic digestion with 40 μl of 2 ng/μl trypsin or chymotrypsin (23). The resulting peptides were extracted and enriched on a reversed-phase C_{18} column (5-μm particle size; 100-μm inside diameter [ID] by 2-cm length [L]; Thermo Fisher Scientific). Peptides were fully resolved on an RP Easy nano-liquid chromatography (LC) C_{18} nanospray column (5-μm particle size; 75-μm ID by 100-mm L) and directly introduced into a Velos PRO Orbitrap mass spectrometer (Thermo Fisher Scientific). Spectra were collected over a *m/z* range of 400 to 2,000 Da using a dynamic exclusion limit of 2 tandem mass spectrometry (MS/MS) spectra of a given peptide mass for 30 s. Compound lists of the resulting spectra were generated using Xcalibur 2.2 software (Thermo Fischer Scientific). MS/MS spectra were searched against the NCBI nonredundant protein database with the *M. leprae* taxonomy filter (1,614 entries) using the Mascot database search engine (version 2.3).

Chymotrypsin digestion of 10 μg of rSodC was performed in 20 μl of 0.1 M ammonium bicarbonate (pH 7.9) at 25°C for 16 h. The resulting peptides were applied to a protein ID chip (Zorbax C_{18}-SB; 5-μm particle size; 75-μm ID by 43-mm L; Agilent Technologies), eluted with an increasing linear gradient of acetonitrile in 0.1% formic acid, introduced directly into an Agilent 6520 quadrupole time-of-flight mass spectrometer at a flow rate of 0.6 ml/min. MS/MS data were collected using ramped collision energies, with the slope of the collision energy set to 3.0 V and an offset of 2.5 V.

Bioinformatics analysis of rSodC. The complete SodC (ML1925) protein sequence was analyzed with the NetOGlyc 3.1 neural network

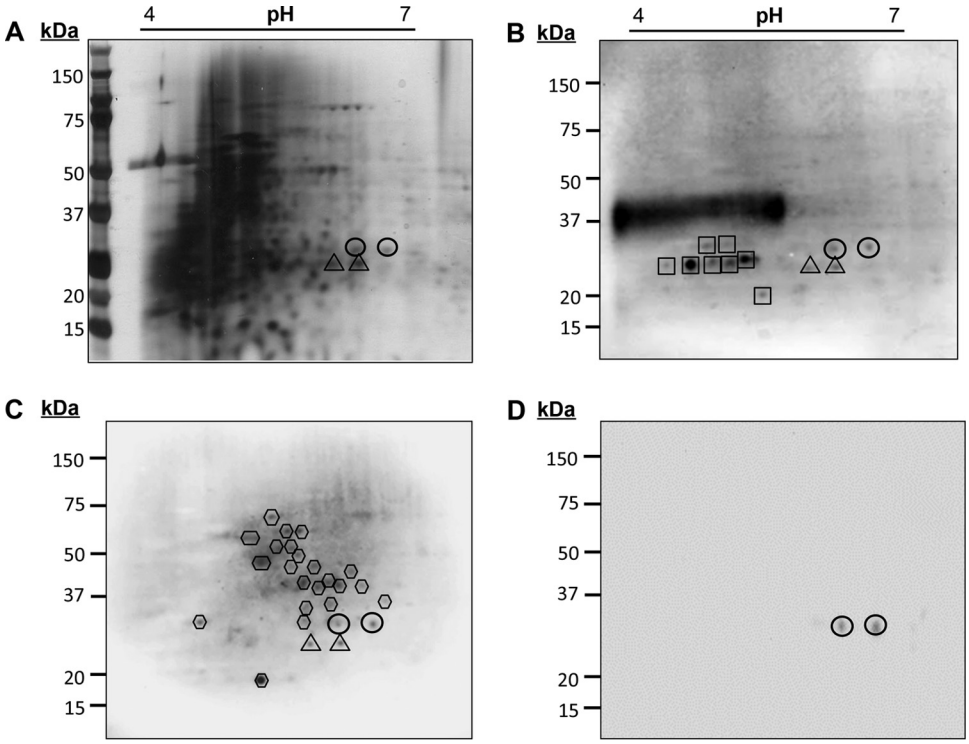

FIG 2 Identification of the langerin-reactive *M. leprae* cell wall glycoprotein SodC. The cell wall protein fraction of *M. leprae* (MLCwA) was resolved by 2D PAGE and silver stained (A) or transferred to PVDF membranes and probed with ConA (B), r-langerin (C), or rabbit anti-SodC polyclonal sera (D). The image for the ConA blot was obtained from 20 s of exposure time and the r-langerin blot from 5 min of exposure time in the ChemiDoc XRS system. Circles and triangles indicate the 2D PAGE locations of *M. leprae* SodC and SodA, respectively. Hexagons designate the other protein spots reactive to r-langerin, and squares designate ConA reactive spots.

(http://www.cbs.dtu.dk/services/NetOGlyc/) for prediction of O-linked glycosylation sites, SignalP 4.1 (http://www.cbs.dtu.dk/services/SignalP/) for the evidence of Sec-dependent secretion signals, and LipoP 1.0 (http://www.cbs.dtu.dk/services/LipoP/) for the cleavage sites of bacterial signal peptidase I and II. Theoretical digestion of SodC protein with chymotrypsin was accomplished with the MS-Digest component of the Protein Prospector program, version 5.10.11 (http://prospector.ucsf.edu/prospector/mshome.htm), with the inclusion of oxidation of methionine as a variable modification and a maximum of three missed cleavages. Theoretical fragmentation patterns of chymotryptic peptides were generated using the MS-Product component of Protein Prospector.

RESULTS

Evaluation of activity of *in vitro* langerin binding to *M. leprae* and *M. tuberculosis* ligands. The CRD of langerin is responsible for binding the Man-α(1→2)-Man at the nonreducing end of glycan chains (8, 24). Therefore, we hypothesized that ManLAM, PIMs, and glycoproteins of *M. leprae* are potential ligands of langerin. Binding of r-langerin to ManLAM of *M. tuberculosis* and *M. leprae*, PIM_6, and MLCwA(−)LAM was assessed using an ILB assay. The binding of r-langerin to immobilized ManLAM of both *Mycobacterium* spp. was significantly less than that of agglutinin. The MLCwA(−)LAM also bound significantly less r-langerin than agglutinin but significantly more than ManLAM (Fig. 1A). The binding of r-langerin to PIM_6 also was significantly less than the binding to agglutinin, and comparison across experiments suggested deceased binding of PIM_6 to langerin compared to ManLAM or MLCwA(−)LAM (Fig. 1A and B). One possible explanation for increased r-langerin binding to MLCwA(−)LAM versus lipoglycans is a lack of available terminal mannose residues in the latter. To assess this possibility, control ILB assays with ConA as the lectin were performed. The levels of ConA binding to *M. tuberculosis* ManLAM and agglutinin or PIM6 and agglutinin were not significantly different, but the level of ConA binding to *M. leprae* ManLAM and MLCwA(−)LAM was significantly less than that of binding to agglutinin or *M. tuberculosis* ManLAM (see Fig. S3 in the supplemental material). The differences between the levels and patterns of ConA and r-langerin binding to the various mycobacterial products provide evidence that low levels of r-langerin binding to the mycobacterial lipoglycans were not due to a lack of terminal mannose residues.

Further assessment of the relative differences in the ability of mycobacterial lipoglycans to bind r-langerin was performed with increasing concentrations of lipoglycans in solution and immobilized r-langerin in an SPR assay. Consistent with results obtained from the langerin ILB assay, the ManLAM of *M. tuberculosis* and *M. leprae* displayed less binding to r-langerin than agglutinin and displayed a dose-dependent response only as the concentration of the ManLAM preparations increased above 10 μg/ml (Fig. 1C). This assay also confirmed that PIM_6 did not act as a ligand for langerin.

Identification of a *M. leprae* glycoprotein SodC as a langerin-reactive ligand. *M. leprae* is known to interact with LCs in human infections; thus, elucidation of the pathogen's cell wall products responsible for the observed r-langerin reactivity was undertaken. Analysis of the MLCwA by 2D PAGE and silver staining revealed a complex profile of proteins (Fig. 2). Western blot analyses of the

TABLE 1 Langerin-reactive *M. leprae* protein candidates identified by LC-MS/MS

ORF (protein)	Enzyme treatment	Peptide sequence[a,b]	Sequence coverage (%)	Protein probability (%)[c]
ML1925 (SodC)	Trypsin	LNAPDGTQVATAK KDGIGTLVTTTDAFTMNDLLAGQK DGIGTLVTTTDAFTMNDLLAGQK TAIIIHAGADNFGNIPPER YSQVNGTPGPDATTISTGDAGKR VACGVIGAD	37	100
	Chymotrypsin	SAGGHFQVPGHTVEPASGNLTSL QVPGHTVEPASGNLTSL TMNDLLAGQKTAIIIHAGADNF SQVNGTPGPDATTISTGDAGKRVACGVIGAD	32	100
ML1172 (MurI)	Trypsin	SSPLLPVGVFDSGVGGLTVAR AIIDQLPDEDIVYVGDTGNGPYGPLSIPEIR AHALAICDDLVGR ILVIACNTASAACLR ERYDVPVVEVILPAVR YDVPVVEVILPAVR TIASHAYQDAFAAARDTEITAVACPR ATIASHAYQDAFAAARDTEITAVACPR QVLGLAEGYLEPLQR VFEATGDPEAFIQLAARFLGPAVSGVQPAR FLGPAVSGVQPAR	62	100
	Chymotrypsin	TVARAIIDQLPDEDIVY EATGDPEAFIQLAARFL AARFLGPAVSGVQPARL GPAVSGVQPARL	17	100

[a] LC-MS/MS data of peptides were searched against the NCBI database using the Mascot or SEQEST algorithms.
[b] The scaffold software 4.0 was used to validate MS/MS-based peptide and protein identifications.
[c] Protein probabilities were assigned by the Protein Prophet algorithm.

MLCwA using ConA as the probe revealed a group of putative, well-resolved glycoproteins at 25 to 30 kDa, as well as a dominant smear at ~37 kDa that is typical of the migration of LAM by 2D PAGE (Fig. 2B). A comparative 2D Western blot of MLCwA probed with r-langerin revealed at least 26 r-langerin-binding protein spots (Fig. 2C). The majority of the r-langerin-reactive protein spots migrated above 37 kDa in a region of the gel with poor resolution or low protein abundance, as determined by silver staining (compare Fig. 2C and A). The r-langerin did not react with LAM, and in the 25- to 30-kDa region, a limited number of the ConA-reactive proteins also bound r-langerin. Specifically, two protein spots at 28 kDa and two protein spots at 25 kDa were observed by probing with ConA and r-langerin (Fig. 2B and C) and could be mapped back to the silver-stained gel. To verify that the r-langerin interaction was via the Ca^{2+}-dependent CRD, an identical 2D blot was probed with r-langerin in the presence of 2 mM EDTA, and inhibition of r-langerin binding was observed (data not shown).

Identification of the four ConA- and r-langerin-reactive *M. leprae* cell wall proteins was achieved by LC-MS/MS analyses of

MSKLAGHRNVAAVTRSALSLSFVAAC$_{26}$VALLSACIQNQPPAT$_{41}$LPGTT
PTVWT$_{51}$GSPAPSGMLGAEAESMGPPNIITRL$_{76}$NAPDGTQVATAKFEF
NNGFATITIATTGVGHLAPGFHGVHIHKVGKCEPSSAGPTGGAPGDFL
SAGGHFQVPGHTVEPASGNLTSLQVRKDGIGTLVTTTDAFTMNDLLA
GQKTAIIIHAGADNFGNIPPERYSQVNGTPGPDATTISTGDAGKRVAC
GVIGAD

FIG 3 Amino acid sequence of *M. leprae* SodC. The sequence represents the putative polypeptide encoded by ML1925. Underlining indicates the predicted signal peptide as defined by LipoP 1.0. The amino acids in bold are sites of O-glycosylation predicted by NetOGlyc. The asterisks indicate predicted chymotrypsin cleavage sites. The section highlighted with the gray box was defined by LC-MS/MS as the region of O-glycosylation.

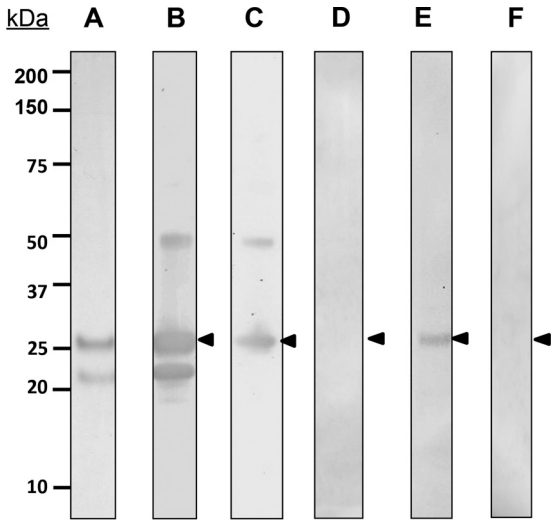

FIG 4 Characterization of rSodC. Purified rSodC produced in *M. smegmatis* was resolved by SDS-PAGE and stained with silver nitrate (A) or transferred to nitrocellulose membrane hybridized to anti-His antibody (B) and PVDF-probed ConA (C) or r-langerin (E). The blot was subjected to reaction with ConA (D) or r-langerin (F) in the presence of 300 mM methylmannoside as the inhibitor. The arrowhead indicates the glycosylated rSodC. The data were reproduced in three individual experiments.

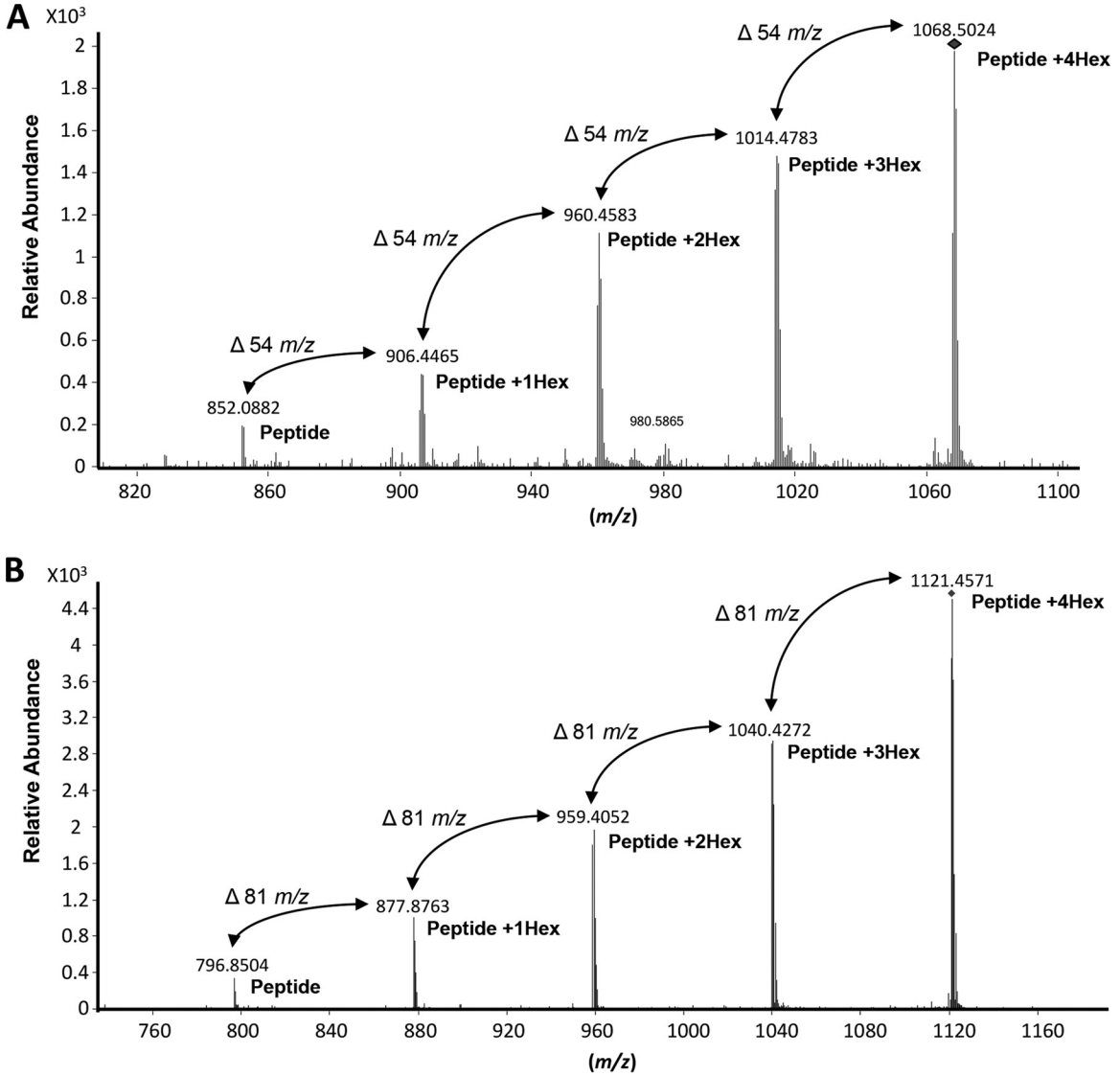

FIG 5 Analysis of peptides derived from rSodC demonstrates protein glycosylation. (A) MS/MS analysis of glycopeptide ($_{51}$TGSPAPSGMLGAEAESMGPPNI ITRL$_{76}$) using low collision energy. MS/MS data were collected using ramped collision energies, with the slope of the collision energy set to 3.0 V and an offset of 2.5 V. All MS/MS data were analyzed using Mascot with the following parameters: a parent ion tolerance of 2.5 Da, a fragment mass tolerance of 1.0 Da, up to two missed cleavages allowed, and variable Met oxidation. The MS/MS was analyzed for the neutral loss of *m/z* of 162.0528 using Mass Hunter Qualitative Analysis software, version B.04.00 (Agilent Technologies). MS/MS fragmentation identified the five most intense $[M + 3H]^{3+}$ ion peaks. These molecular ions (*m/z* 852.0882, 906.4465, 960.4583, 1,014.4783, and 1,068.5024) differed by 54 *m/z*, corresponding to hexose residues of a triply charged mass of the glycopeptide. (B) MS/MS analysis of glycopeptide ($_{51}$TGSPAPSGMLGAEAESM$_{67}$) using low collision energy. MS/MS fragmentation identified the five most intense $[M + 2H]^{2+}$ ion peaks. These molecular ions (*m/z* 796.8504, 877.8763, 959.4052, 1,040.4272, and 1,121.4571) differed by 81 *m/z* corresponding hexose residues of a doubly charged mass of the glycopeptide. The 1,068.5024 and 1,121.4571 *m/z* ions of the respective glycopeptides were subjected to *de novo* sequence analysis to confirm identity of the glycopeptide using high-collision-energy fragmentation (Fig. 6).

peptides generated by trypsin and chymotrypsin digestions of the excised protein spots. Given the minor abundance of the targeted protein spots, gel pieces were also cut from nearby unstained regions of the same gels and used as a negative control. The LC-MS/MS analyses identified five proteins in the excised 2D-PAGE spots that migrated at 28 kDa (ML0072, SodA; ML0381, GroEL-1; ML0773, MtrA; ML1172; MurI; and ML1925, SodC). Peptides of SodA were also detected in analysis of the negative-control gel pieces. Previous proteomics studies of *M. leprae* discovered that MtrA, SodA, and GroEL-1 are predominant proteins in the cell wall fractions (15). Thus, they were suspected as contaminants of the 28-kDa r-langerin 2D-gel spots. The SodC and MurI were identified with sequence coverage of 37% and 66%, respectively (Table 1). Bioinformatics analyses of these two proteins indicated that SodC was a translocated protein with predicted glycosylation sites in the N- and C-terminal regions of the mature protein (Fig. 3). In contrast, MurI lacked predicted sites of glycosylation and a translocation signal sequence. Rabbit polyclonal antisera was raised against a recombinant form of SodC produced in *E. coli* and used to probe a 2D Western blot of MLCwA to verify that the targeted 28-kDa protein spots recognized by the r-langerin and ConA truly contained SodC (Fig. 2D).

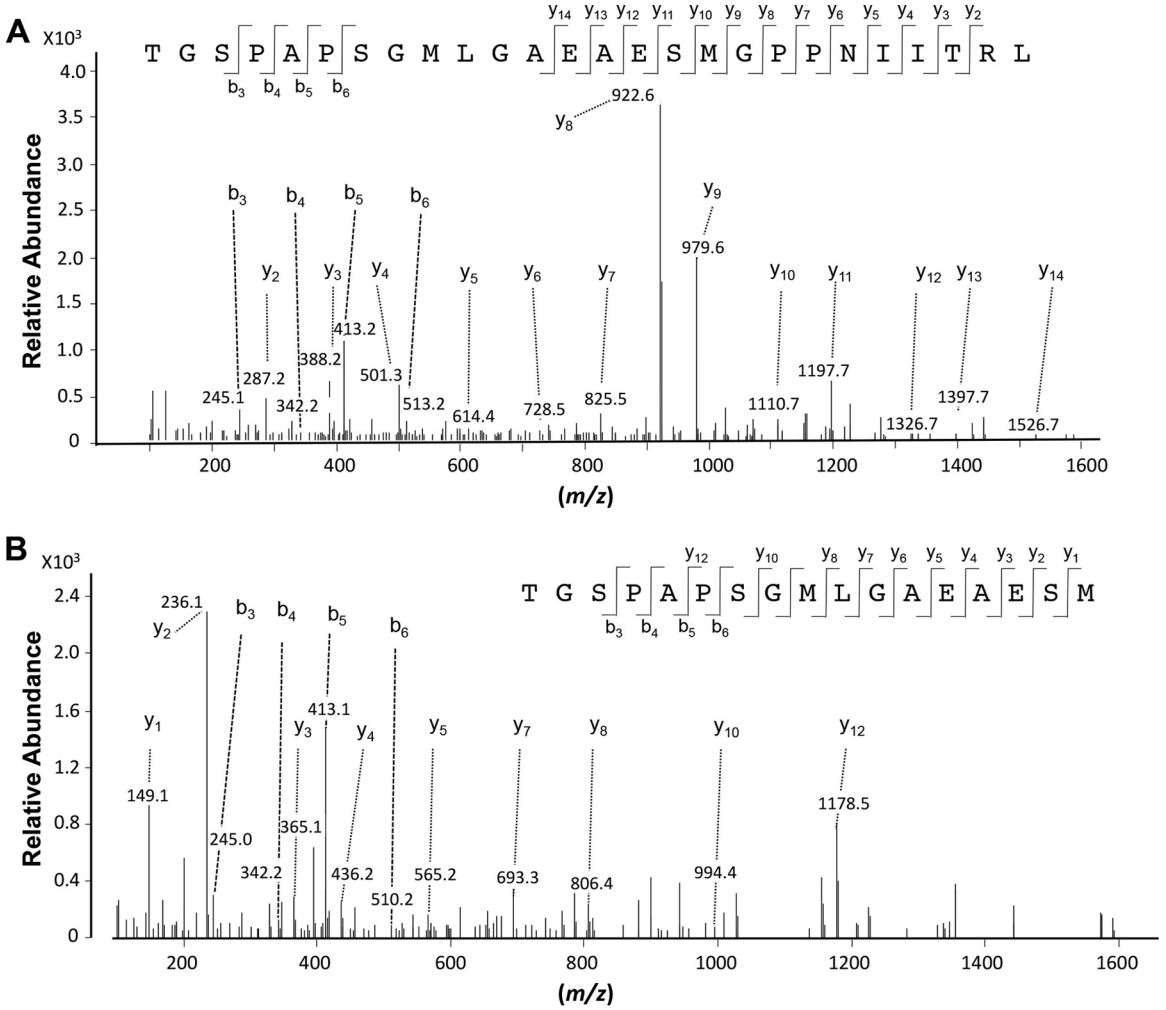

FIG 6 MS/MS fragmentation and confirmation of the amino acid sequence of the *M. leprae* rSodC glycopeptides. (A) The MS/MS fragmentation of 1,068.5024 *m/z* $(M + 3H)^{3+}$ corresponding to the $_{51}$TGSPAPSGMLGAEAESMGPPNIITRL$_{76}$ glycopeptide (Fig. 5A) obtained with a collision energy of 42.0 eV provided *b* and *y* series ions that confirmed the amino acid sequence of the peptide. (B) MS/MS of the 1,121.4571 *m/z* $(M + 2H)^{2+}$ corresponding to the $_{51}$TGSPAPSGM LGAEAESM$_{67}$ glycopeptide (Fig. 5B) obtained with a collision energy of 44.0 eV provided *b* and *y* series ions that confirmed the amino acid sequence of the peptide. MS/MS ion data were deconvoluted using the Mass Hunter Qualitative Analysis software, version B.04.00, and the amino acid caliper was used to identify the probable amino acid fragmentation differences between the dominant ions in the spectra.

SodA, GroEL1, and PhoY (ML2188) were dominantly identified in the spots that migrated at 25 kDa and exhibited 67%, 27%, and 40% of sequence coverage, respectively. No evidence for glycosylation and secretion signals was found in protein sequences of SodA, GroEL1, and PhoY by bioinformatic analyses. Thus, further analyses were directed at the 28-kDa SodC.

Characterization of rSodC and verification of glycosylation. *M. smegmatis* possesses the enzymatic machinery to posttranslationally modify proteins and can be used as a heterologous host for production of recombinant glycoproteins of *M. tuberculosis* and *M. leprae* (17). Therefore, a glycosylated recombinant form of the *M. leprae* SodC (rSodC) was produced in *M. smegmatis*. Analysis of rSodC after purification by IMAC and prior to final purification by preparative SDS-PAGE demonstrated two anti-His antibody-reactive protein bands at ~20 and 25 kDa. However, only the 25-kDa product reacted to ConA and r-langerin, and methylmannoside inhibited both of these lectin interactions (Fig. 4). This pattern of antibody and lectin reactivity indicated that the N-terminal portion of the 25-kDa rSodC protein was glycosylated and was lost by proteolysis, resulting in the 20-kDa product. This same phenomenon of proteolytic processing after posttranslational modification also was observed in the analysis of rSodC of *M. tuberculosis* (23). After final purification by preparative SDS-PAGE elution, the 25-kDa rSodC retained ConA and r-langerin reactivity (see Fig. S4 in the supplemental material).

As noted above, bioinformatics analyses of the *M. leprae* SodC revealed predicted glycosylation sites within theoretical chymotryptic peptides (Fig. 3). To confirm glycosylation of rSodC, the protein was subjected to digestion with chymotrypsin and the resulting peptides were analyzed by LC-electrospray ionization (ESI)-MS/MS. The MS/MS fragmentation of the peptides with a collision energy of 13.0 to 13.7 V was used to interrogate peptides for neutral losses corresponding to the mass of a hexose unit (*m/z* 162.05) (23). This identified two peptide ions (*m/z* 1,068.5024 $[M + 3H]^{3+}$ and *m/z* 1,121.4571 $[M + 2H]^{2+}$) as potential glycopeptides, and evaluation of the MS/MS data indicated that both

peptides were modified with four hexose residues (Fig. 5). The smallest major fragment ions for these two peptides (*m/z* 852.0882 $[M + 3H]^{3+}$ and *m/z* 796.8504 $[M + 2H]^{2+}$) were predicted to be the nonglycosylated forms of the *m/z* 1,068.5024 and *m/z* 1,121.4571 parent ions, respectively. These two nonglycosylated fragment ions mapped to the N terminus of the rSodC, specifically, Thr_{51}-Leu_{76} for *m/z* 852.0882 and Thr_{51}-Met_{67} for *m/z* 796.8504. To confirm the location of these two glycopeptides within rSodC, MS/MS analyses of the 1,068.5024 $[M + 3H]^{3+}$ and *m/z* 1,121.4571 $[M + 2H]^{2+}$ parent ions were performed with a higher collision energy to fragment the peptide backbone (Fig. 6). Within the rSodC glycopeptide region, three amino acids were predicted to be glycosylated (Thr_{51}, Ser_{53}, and Ser_{57}) (Fig. 3).

Previous characterization of rSodC of *M. tuberculosis* revealed that the majority of the protein had been further modified such that the N-terminal acylation was removed or the protein was processed via signal peptidase I (23). Thus, the purified rSodC of *M. leprae* was subjected to N-terminal sequencing. These data indicated that at least a portion of the recombinant product had an N-terminal sequence of Thr-Leu-Pro. This corresponds to amino acids 41 to 43 of *M. leprae* SodC (Fig. 3) and to the predicted mature N terminus if the protein is processed via signal peptidase I during translocation. However, bioinformatics analyses also predict Cys_{26} as the mature N terminus if the protein is processed by signal peptidase II and acylated. To address whether two potential forms of rSodC were present and whether these different forms responded to r-langerin similarly, the recombinant product was subjected to TX-114 biphasic partitioning. Approximately 27.1% of the total protein recovered partitioned to the detergent phase. Thus, the majority of the rSodC appeared to be nonacylated. A comparative analysis of the r-langerin interaction of each protein preparation via an SPR assay revealed that acylated (TX-114 detergent) forms of rSodC bound to r-langerin in a dose-dependent manner, but with less reactivity than the nonacylated (TX-114 aqueous) form and unfractioned SodC (Fig. 7).

Langerin affinity analysis of rSodC and *M. leprae* ManLAM. To compare the relative affinity of r-langerin to purified rSodC versus ManLAM, SPR analyses were performed with r-langerin immobilized to the biosensor and reacted with various concentrations of rSodC (50 to 3,200 nM) and *M. leprae* ManLAM (400 to 6,400 nM). The sensograms obtained demonstrated a dominant interaction of r-langerin with rSodC compared to *M. leprae* ManLAM (Fig. 8). Specifically, equilibrium dissociation constants (K_D) of rSodC and *M. leprae* ManLAM were determined to be 0.862 μM and 18.69 μM, respectively (Fig. 8C and D). Moreover, the K_D of *M. leprae* ManLAM had to be estimated, as a binding equilibrium was not achieved with the concentration of analyte used. A comparison of the SPR sensogram of rSodC (Fig. 8A) to that of the control soybean agglutinin (see Fig. S2A in the supplemental material) for r-langerin binding indicated these two ligands yielded similar binding and dissociation kinetics. However, the soybean agglutinin demonstrated a higher affinity, with a K_D of 0.187 μM. A second control ligand, yeast invertase, had higher affinity (K_D of 0.035 μM) and prolonged dissociation, indicating high avidity (see Fig. S2B in the supplemental material). Further analysis of the rSodC and *M. leprae* ManLAM SPR data was performed using Scatchard plots to assess the langerin-analyte interactions in a saturated-receptor-binding state. A straight Scatchard line was observed for the rSodC–r-langerin interaction, indicating a 1:1 ligand-to-receptor binding (25) (Fig. 8C). In contrast, the

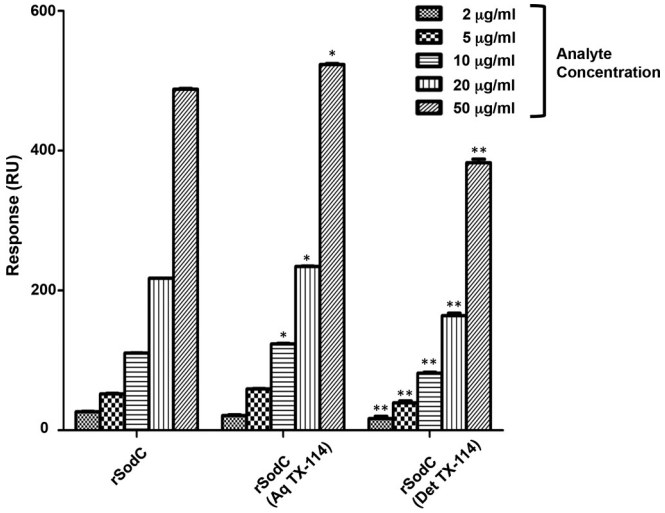

FIG 7 r-langerin binding to rSodC, rSodC (Aq TX-114), and rSodC (Det TX-114) as measured by SPR. The dose responses of purified rSodC, rSodC enriched in the TX-114 aqueous phase, rSodC (Aq TX-114), and rSodC enriched in the TX-114 detergent phase, rSodC (Det TX-114) interacting with immobilized r-langerin were measured by SPR. A one-way ANOVA combined with Tukey's multiple comparison analysis was performed to determine the statistical difference between the various forms of rSodC. **, $P < 0.01$ for rSodC (Det TX-114) versus rSodC and rSodC (Aq TX-114); *, $P < 0.01$ for rSodC (Aq TX-114) versus rSodC.

Scatchard plot of the *M. leprae* ManLAM–r-langerin binding could not be fitted to a straight line but rather resembled a sigmoid curve that would be interpreted as heterogeneous receptor affinity (25). This was also consistent with the observation that ManLAM did not interact with langerin in a dose-dependent manner until the concentration was raised above 1,600 nM.

DISCUSSION

This report provides biochemical evidence that langerin, the major C-type lectin on the surface of LCs, directly reacts to glycoconjugates of *M. leprae* and for the first time defines bacterial ligands of langerin. Surprisingly, the dominant lipoglycans of *M. leprae* ManLAM and particularly PIM_6 appeared to interact less well under the condition of the assays used. However, glycoproteins in the cell envelope of this bacterium demonstrated binding to langerin that was similar to that of the control ligand, agglutinin. Multiple mycobacterial glycoproteins have been identified and characterized, and all are presumed to possess short α(1→2) or α(1→3) oligosaccharides of mannose, as found with the *M. tuberculosis* Apa (45 kDa) and *M. bovis* MPB83 glycoproteins, respectively (5, 26). Native *M. tuberculosis* glycoproteins are easily purified; however, the purification of native *M. leprae* glycoproteins is limited by the necessity of *in vivo* growth. Our laboratory and others established that the *M. tuberculosis* gene products Rv1002c (Pmt1) and Rv1159 (PimE) are responsible for the modification of *M. tuberculosis* proteins with mannose and α(1→2) oligomannose structures (27, 28). Bioinformatics analyses provide strong evidence that *M. leprae* possesses full-length and functional homologues of Pmt1 (ML0192) and PimE (ML1504), suggesting that *M. leprae* protein mannosylation machinery is functional (29). Our data demonstrating ConA and langerin binding to a subset of *M. leprae* native cell wall proteins has now provided experimental evidence of a functional protein glycosylation system in this bac-

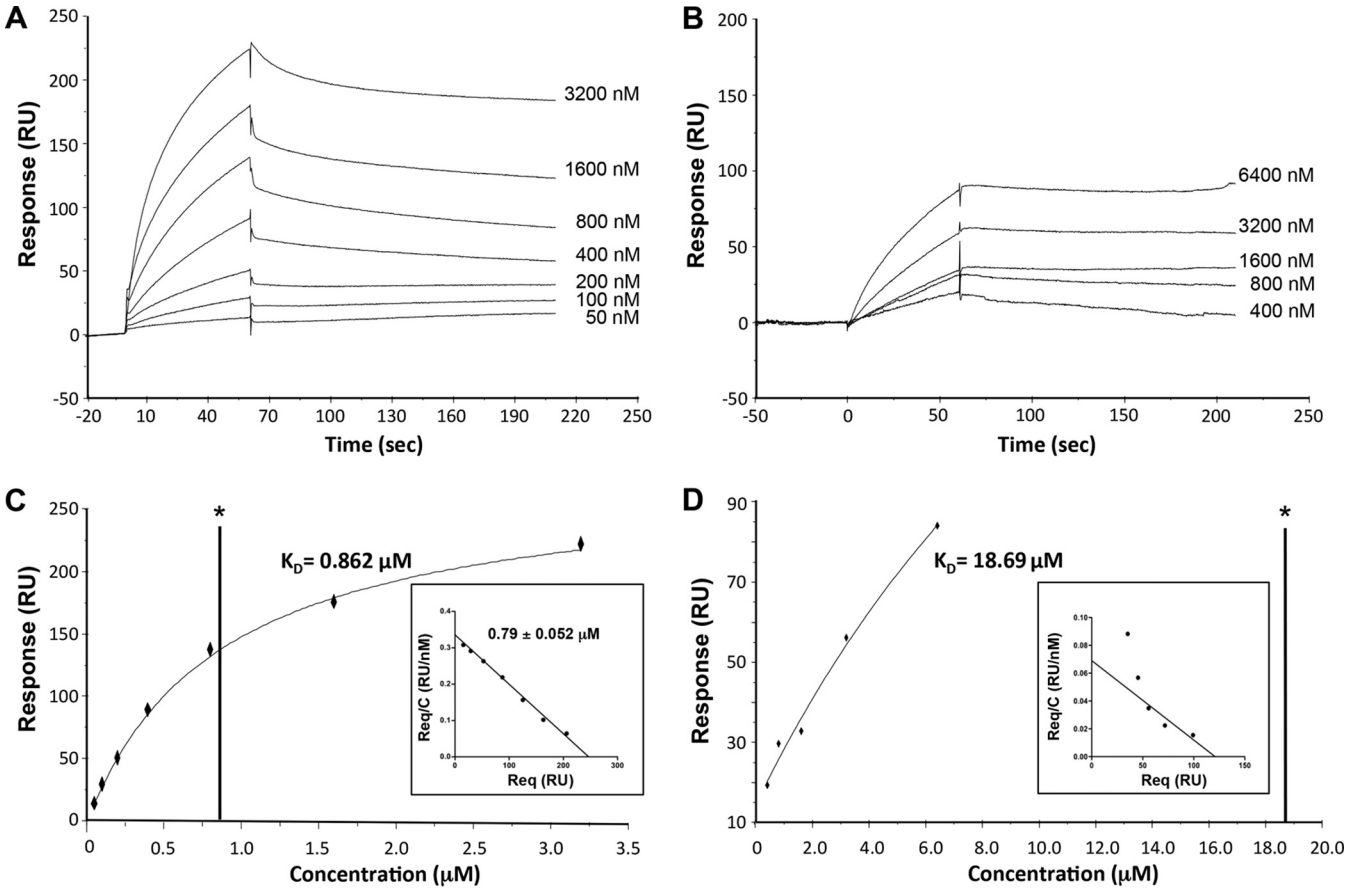

FIG 8 r-langerin affinity to rSodC and *M. leprae* ManLAM as measured by SPR. r-langerin interaction on the sensor chip was evaluated using a range of rSodC concentrations from 50 to 3,200 nM (A) and *M. leprae* ManLAM from 400 to 6,400 nM (B). The binding affinity (K_D) of rSodC (C) and *M. leprae* ManLAM (D) to r-langerin were obtained from steady-state affinity measurements. The lines denoted by an asterisk indicate the calculated or predicted K_D. The insets depict the Scatchard plot of saturation binding of rSodC and *M. leprae* ManLAM to r-langerin.

terium and led to the identification of *M. leprae* SodC as at least one of the ligands of langerin presumptively glycosylated with mannose residues.

Production of a recombinant form of *M. leprae* SodC in *M. smegmatis* and analysis by LC-MS/MS confirmed glycosylation of the protein and identified a 26-amino-acid peptide (T_{51} to L_{76}) that contained four hexose residues. Further, one Thr and two Ser residues in this region were predicted to be O-glycosylation sites. This N-terminal glycopeptide region of *M. leprae* SodC was consistent with the sites of glycosylation identified in the *M. tuberculosis* SodC homologue (23). The mature N terminus of the *M. leprae* SodC is predicted to be a lipoprotein with a mature N terminus and site of acylation at C_{26}. There are three additional predicted sites of glycosylation in the C_{26}-to-W_{50} peptide. However, the LC-MS/MS analyses failed to identify any peptide for this region. N-terminal sequencing and TX-114 biphasic partitioning suggested that the acylated form of rSodC was only a small proportion of the total purified protein. Thus, the inability to detect the N-terminal acylated peptide may reflect the low abundance of the acylated rSodC and the refractivity of the acylated peptide to efficient ionization or elution with the reversed-phase chromatography methods applied.

The 2D Western blot analyses that led to characterization of *M. leprae* SodC also indicted a number of other potential *M. leprae* protein ligands of langerin. SodA was detected as the major product of the 25-kDa langerin-reactive protein spots, and GroEL1 (presumably as degradation products of this protein) was detected in both the 28- and 25-kDa protein spots. SodA has been reported to specifically bind to surface of human respiratory epithelial cells (30), and *M. bovis* GroEL1 was shown to be DC-SIGN ligands (31). Although bioinformatics indicated that these two proteins are not glycosylated, their possible interaction with langerin in a carbohydrate-independent manner cannot be excluded. Given the number of potential langerin targets, the possibility of carbohydrate independent interactions, and the limited availability of *M. leprae* products, a proteomics approach directed at the capture and identification of langerin-reactive peptides is under way to identify all potential *M. leprae* ligands of langerin.

The molecular interaction of rSodC-langerin revealed a 1:1 binding model that was similar to the r-langerin interactions with agglutinin but greatly different from the high-avidity interaction of r-langerin with yeast invertase. Unlike the relatively simple mannosylation of the mycobacterial glycoproteins, yeast invertase is substituted with a highly branched mannan structure and fits the binding model observed between langerin and the trimeric multivalent form of the envelope gp140 of HIV (32) and highly branched neoglycoproteins (33). Thus, the level of glycosylation observed on the rSodC was in concordance with the kinetics of

this protein's binding to r-langerin. However, the increased binding efficiency of the glycosylated rSodC to langerin compared to that of ManLAM was unexpected given the highly branched structure of ManLAM and number of terminal mannose residues. ManLAM and PIM_6 are known ligands of other C-type lectins (e.g., DC-SIGN, human pulmonary surfactant protein A, and mannose receptor) (12, 34–37). Previously, the acyl functions of ManLAM were found to play a critical role in recognition by human pulmonary surfactant protein A and DC-SIGN, presumably by allowing micelle formation of ManLAM at higher concentrations (36). We also observed that higher concentrations of ManLAM (>1,600 nM) were required to bind with r-langerin. This indicated that langerin recognition of the collective mannose residues of ManLAM may be dependent on the conformation of the ligand. The sigmoidal Scatchard plot curve for the ManLAM and r-langerin binding indicated heterogeneous interactions that also could be associated with ManLAM, assuming different conformations at low and high concentrations. Interestingly, although the detergent-phase (acylated) version of rSodC did not show the same type of bimodal dose response as ManLAM, it was less reactive to immobilized r-langerin than the aqueous phase (nonacylated) rSodC. Thus, the acylation of rSodC may impact langerin binding in a different manner. PIM_6 possesses a terminal Man-$\alpha(1\rightarrow2)$-Man; despite this, r-langerin failed to recognize PIM_6 in either the ILB or SPR assay independent of the ligand concentration, suggesting that the terminal mannose residue of PIM_6 was not accessible to the CRD of langerin.

Previous studies of C-type lectin specificities also may contribute to the observations of differential langerin binding to *M. leprae* SodC and ManLAM. Holla and Skerra (8) demonstrated that the monomeric CRD of langerin has a preference for terminal mannose residues of linear and short glycans. This is in contrast to the high affinity of DC-SIGN to most oligomannosides and a binding preference for highly branched mannosylated saccharides. Structural studies with the langerin CRD also indicate a preferential binding of specific glycans rather than broad specificity associated with other C-type lectins (24). Thus, we speculate that specific oligosaccharide lengths or linkages present on mycobacterial glycoproteins and other glycoconjugates may imply C-type lectin specificity. Alternatively, it is possible that the specificity of trimeric langerin is based on spatial distribution of the glycosylation sites on the polypeptide backbone of SodC.

LCs are predominant in lesions of tuberculoid-leprosy patients compared to those of lepromatous-leprosy patients and are involved in blocking *M. leprae* dissemination at the site of infection (2, 38, 39). This along with the presentation of *M. leprae* antigens in a langerin-dependent manner (2) indicates an important role for LCs in the pathogenesis of leprosy. The identification of *M. leprae* SodC as a ligand of langerin provides a basis for future experimentation that addresses langerin-mediated interactions of LCs with *M. leprae*. However, it must be recognized that other factors, such as relative concentration and availability of individual ligands at the cell surface, will influence their contribution to the ability of *M. leprae* to bind langerin *in vivo*. Experiments to assess the relative contribution of ManLAM and SodC are ongoing and are being extended to new ligands as they are identified and characterized. Further, knowledge of the native structure of the *M. leprae* glycoconjugates and elucidation of specific interactions with langerin and the C-type lectins of other host cells will provide the ability to assess the biological significance of individual C-type lectin interactions at the various stages of leprosy.

ACKNOWLEDGMENTS

This study was supported by NIH, NIAID grants R01-AI022553, R01-AI047868, and R01-AI082575 and NIAMS (NIH) grants P50-AR063020 and R01-AR040312.

We thank Brian Cranmer for technical assistance in performing LC-MS/MS analyses.

REFERENCES

1. **Jacobson RR, Krahenbuhl JL.** 1999. Leprosy. Lancet **353:**655–660. http://dx.doi.org/10.1016/S0140-6736(98)06322-3.
2. **Hunger RE, Sieling PA, Ochoa MT, Sugaya M, Burdick AE, Rea TH, Brennan PJ, Belisle JT, Blauvelt A, Porcelli SA, Modlin RL.** 2004. Langerhans cells utilize CD1a and langerin to efficiently present nonpeptide antigens to T cells. J Clin Invest **113:**701–708. http://dx.doi.org/10.1172/JCI19655.
3. **Rambukkana A.** 2010. Usage of signaling in neurodegeneration and regeneration of peripheral nerves by leprosy bacteria. Prog Neurobiol **91:**102–107. http://dx.doi.org/10.1016/j.pneurobio.2009.12.002.
4. **Krutzik SR, Tan B, Li H, Ochoa MT, Liu PT, Sharfstein SE, Graeber TG, Sieling PA, Liu Y-J, Rea TH, Bloom BR, Modlin RL.** 2005. TLR activation triggers the rapid differentiation of monocytes into macrophages and dendritic cells. Nat Med **11:**653–660. http://dx.doi.org/10.1038/nm1246.
5. **Dobos KM, Swiderek K, Khoo KH, Brennan PJ, Belisle JT.** 1995. Evidence for glycosylation sites on the 45-kilodalton glycoprotein of *Mycobacterium tuberculosis*. Infect Immun **63:**2846–2853.
6. **Brennan PJ, Nikaido H.** 1995. The envelope of mycobacteria. Annu Rev Biochem **64:**29–63. http://dx.doi.org/10.1146/annurev.bi.64.070195.000333.
7. **Geijtenbeek TBH, Gringhuis SI.** 2009. Signalling through C-type lectin receptors: shaping immune responses. Nat Rev Immunol **9:**465–479. http://dx.doi.org/10.1038/nri2569.
8. **Holla A, Skerra A.** 2011. Comparative analysis reveals selective recognition of glycans by the dendritic cell receptors DC-SIGN and Langerin. Protein Eng Des Sel **24:**659–669. http://dx.doi.org/10.1093/protein/gzr016.
9. **Mitchell DA, Fadden AJ, Drickamer K.** 2001. A novel mechanism of carbohydrate recognition by the C-type lectins DC-SIGN and DC-SIGNR. Subunit organization and binding to multivalent ligands. J Biol Chem **276:**28939–28945.
10. **Stambach NS, Taylor ME.** 2003. Characterization of carbohydrate recognition by langerin, a C-type lectin of Langerhans cells. Glycobiology **13:**401–410. http://dx.doi.org/10.1093/glycob/cwg045.
11. **Gringhuis SI, den Dunnen J, Litjens M, van der Vlist M, Geijtenbeek TBH.** 2009. Carbohydrate-specific signaling through the DC-SIGN signalosome tailors immunity to *Mycobacterium tuberculosis*, HIV-1 and *Helicobacter pylori*. Nat Immunol **10:**1081–1088. http://dx.doi.org/10.1038/ni.1778.
12. **Torrelles JB, Azad AK, Schlesinger LS.** 2006. Fine discrimination in the recognition of individual species of phosphatidyl-myo-inositol mannosides from *Mycobacterium tuberculosis* by C-type lectin pattern recognition receptors. J Immunol **177:**1805–1816. http://dx.doi.org/10.4049/jimmunol.177.3.1805.
13. **Pitarque S, Herrmann J-L, Duteyrat J-L, Jackson M, Stewart GR, Lecointe F, Payre B, Schwartz O, Young DB, Marchal G, Lagrange PH, Puzo G, Gicquel B, Nigou J, Neyrolles O.** 2005. Deciphering the molecular bases of *Mycobacterium tuberculosis* binding to the lectin DC-SIGN reveals an underestimated complexity. Biochem J **392:**615–624. http://dx.doi.org/10.1042/BJ20050709.
14. **Shepard CC, Draper P, Rees RJ, Lowe C.** 1980. Effect of purification steps on the immunogenicity of *Mycobacterium leprae*. Br J Exp Pathol **61:**376–379.
15. **Marques MA, Chitale S, Brennan PJ, Pessolani MC.** 1998. Mapping and identification of the major cell wall-associated components of *Mycobacterium leprae*. Infect Immun **66:**2625–2631.
16. **Bordier C.** 1981. Phase separation of integral membrane proteins in Triton X-114 solution. J Biol Chem **256:**1604–1607.
17. **Sieling PA, Hill PJ, Dobos KM, Brookman K, Kuhlman AM, Fabri M, Krutzik SR, Rea TH, Heaslip DG, Belisle JT, Modlin RL.** 2008. Con-

served mycobacterial lipoglycoproteins activate TLR2 but also require glycosylation for MHC class II-restricted T cell activation. J Immunol **180:** 5833–5842. http://dx.doi.org/10.4049/jimmunol.180.9.5833.

18. **Covert BA, Spencer JS, Orme IM, Belisle JT.** 2001. The application of proteomics in defining the T cell antigens of *Mycobacterium tuberculosis*. Proteomics **1:**574–586. http://dx.doi.org/10.1002/1615-9861(200104)1:4<574::AID-PROT574>3.0.CO;2-8.
19. **Kim HJ, Prithiviraj K, Groathouse N, Brennan PJ, Spencer JS.** 2013. Gene expression profile and immunological evaluation of unique hypothetical unknown proteins of *Mycobacterium leprae* by using quantitative real-time PCR. Clin Vaccine Immunol **20:**181–190. http://dx.doi.org/10.1128/CVI.00419-12.
20. **Tada Y, Riedl E, Lowenthal MS, Liotta LA, Briner DM, Crouch EC, Udey MC.** 2006. Identification and characterization of endogenous langerin ligands in murine extracellular matrix. J Investig Dermatol **126:** 1549–1558. http://dx.doi.org/10.1038/sj.jid.5700283.
21. **Spencer JS, Kim HJ, Wheat WH, Chatterjee D, Balagon MV, Cellona RV, Tan EV, Gelber R, Saunderson P, Duthie MS, Reece ST, Burman W, Belknap R, Kenzie WR, Geluk A, Oskam L, Dockrell HM, Brennan PJ.** 2011. Analysis of antibody responses to *Mycobacterium leprae* phenolic glycolipid I, lipoarabinomannan, and recombinant proteins to define disease subtype-specific antigenic profiles in leprosy. Clin Vaccine Immunol **18:**260–267. http://dx.doi.org/10.1128/CVI.00472-10.
22. **Lozach P-Y, Lortat-Jacob H, de Lacroix de Lavalette A, Staropoli I, Foung S, Amara A, Houlès C, Fieschi F, Schwartz O, Virelizier J-L, Arenzana-Seisdedos F, Altmeyer R.** 2003. DC-SIGN and L-SIGN are high affinity binding receptors for hepatitis C virus glycoprotein E2. J Biol Chem **278:**20358–20366. http://dx.doi.org/10.1074/jbc.M301284200.
23. **Sartain MJ, Belisle JT.** 2009. N-terminal clustering of the O-glycosylation sites in the *Mycobacterium tuberculosis* lipoprotein SodC. Glycobiology **19:**38–51. http://dx.doi.org/10.1093/glycob/cwn102.
24. **Feinberg H, Taylor ME, Razi N, McBride R, Knirel YA, Graham SA, Drickamer K, Weis WI.** 2011. Structural basis for langerin recognition of diverse pathogen and mammalian glycans through a single binding site. J Mol Biol **405:**1027–1039. http://dx.doi.org/10.1016/j.jmb.2010.11.039.
25. **Wofsy C, Goldstein B.** 1992. Interpretation of Scatchard plots for aggregating receptor systems. Math Biosci **112:**115–154. http://dx.doi.org/10.1016/0025-5564(92)90090-J.
26. **Michell SL, Whelan AO, Wheeler PR, Panico M, Easton RL, Etienne AT, Haslam SM, Dell A, Morris HR, Reason AJ, Herrmann JL, Young DB, Hewinson RG.** 2003. The MPB83 antigen from *Mycobacterium bovis* contains O-linked mannose and (1→3)-mannobiose moieties. J Biol Chem **278:**16423–16432. http://dx.doi.org/10.1074/jbc.M207959200.
27. **Liu C-F, Tonini L, Malaga W, Beau M, Stella A, Bouyssié D, Jackson MC, Nigou J, Puzo G, Guilhot C, Burlet-Schiltz O, Rivière M.** 2013. Bacterial protein-O-mannosylating enzyme is crucial for virulence of *Mycobacterium tuberculosis*. Proc Nat Acad Sci U S A **110:**6560–6565. http://dx.doi.org/10.1073/pnas.1219704110.
28. **VanderVen BC, Harder JD, Crick DC, Belisle JT.** 2005. Export-mediated assembly of mycobacterial glycoproteins parallels eukaryotic pathways. Science **309:**941–943. http://dx.doi.org/10.1126/science.1114347.
29. **Kaur D, Guerin ME, Skovierová H, Brennan PJ, Jackson M.** 2009. Biogenesis of the cell wall and other glycoconjugates of *Mycobacterium tuberculosis*. Adv Appl Microbiol **69:**23–78. http://dx.doi.org/10.1016/S0065-2164(09)69002-X.
30. **Reddy VM, Kumar B.** 2000. Interaction of *Mycobacterium avium* complex with human respiratory epithelial cells. J Infect Dis **181:**1189–1193. http://dx.doi.org/10.1086/315327.
31. **Carroll MV, Sim RB, Bigi F, Jäkel A, Antrobus R, Mitchell DA.** 2010. Identification of four novel DC-SIGN ligands on *Mycobacterium bovis* BCG. Protein Cell **1:**859–870. http://dx.doi.org/10.1007/s13238-010-0101-3.
32. **Hijazi K, Wang Y, Scala C, Jeffs S, Longstaff C, Stieh D, Haggarty B, Vanham G, Schols D, Balzarini J, Jones IM, Hoxie J, Shattock R, Kelly CG.** 2011. DC-SIGN increases the affinity of HIV-1 envelope glycoprotein interaction with CD4. PLoS One **6:**e28307. http://dx.doi.org/10.1371/journal.pone.0028307.
33. **Quétard C, Bourgerie S, Normand-Sdiqui N, Mayer R, Strecker G, Midoux P, Roche AC, Monsigny M.** 1998. Novel glycosynthons for glycoconjugate preparation: oligosaccharylpyroglutamylanilide derivatives. Bioconj Chem **9:**268–276. http://dx.doi.org/10.1021/bc970122p.
34. **Maeda N, Nigou J, Herrmann J-L, Jackson M, Amara A, Lagrange PH, Puzo G, Gicquel B, Neyrolles O.** 2003. The cell surface receptor DC-SIGN discriminates between *Mycobacterium* species through selective recognition of the mannose caps on lipoarabinomannan. J Biol Chem **278:** 5513–5516. http://dx.doi.org/10.1074/jbc.C200586200.
35. **Schlesinger LS, Hull SR, Kaufman TM.** 1994. Binding of the terminal mannosyl units of lipoarabinomannan from a virulent strain of Mycobacterium tuberculosis to human macrophages. J Immunol **152:**4070–4079.
36. **Rivière M, Moisand A, Lopez A, Puzo G.** 2004. Highly ordered supramolecular organization of the mycobacterial lipoarabinomannans in solution. evidence of a relationship between supra-molecular organization and biological activity. J Mol Biol **344:**907–918. http://dx.doi.org/10.1016/j.jmb.2004.09.092.
37. **Sidobre S, Puzo G, Rivière M.** 2002. Lipid-restricted recognition of mycobacterial lipoglycans by human pulmonary surfactant protein A: a surface-plasmon-resonance study. Biochem J **365:**89–97. http://dx.doi.org/10.1042/BJ20011659.
38. **Gimenez MF, Gigli I, Tausk FA.** 1989. Differential expression of Langerhans cells in the epidermis of patients with leprosy. Br J Dermatol **121:** 19–26. http://dx.doi.org/10.1111/j.1365-2133.1989.tb01395.x.
39. **Miranda A, Amadeu TP, Schueler G, Alvarenga FBF, Duppré N, Ferreira H, Nery JAC, Sarno EN, Duppre N.** 2007. Increased Langerhans cell accumulation after mycobacterial stimuli. Histopathology **51:**649–656. http://dx.doi.org/10.1111/j.1365-2559.2007.02848.x.